Visible electroluminescence from silicon nanocrystals embedded in amorphous silicon nitride matrix

Liang-Yih Chen,[a] Wen-Hua Chen, and Franklin Chau-Nan Hong[b]
Department of Chemical Engineering and Center for Micro-Nano Technology, National Cheng Kung University, 1 University Road, Tainan, Taiwan, Republic of China

(Received 14 October 2004; accepted 24 March 2005; published online 5 May 2005)

Visible electroluminescence from silicon nanocrystals (Si-NCs) embedded in amorphous silicon nitride (a-SiN_x) films has been observed. The Si-NC/a-SiN_x films were deposited by evaporating silicon from electron gun into the inductively coupled plasma of nitrogen. The density of Si-NCs in the a-SiN_x matrix was around 10^{12} cm^{-2}. Strong room temperature photoluminescence was observed in 2.8 and 3.0 eV, different from literature values. The electroluminescence (EL) devices were fabricated with Si-NCs/a-SiN_x film as the active layer using the Al or Ca/Ag cathode and the indium tin oxide anode. Through tunneling, the electrons and holes were respectively injected from the cathode and anode into Si-NCs and confined within Si-NCs for light emission by the high band gap a-SiN_x matrix. For the device with Ca/Ag cathode, the turn-on voltage was as low as 10 V and the EL efficiency was about 1.6×10^{-1} Cd/A. The EL spectra consisted of two broad peaks centered around 2.5 and 2.8 eV. Our results demonstrate that Si-NCs/a-SiN_x nanocomposite films have potentials to be fabricated into electroluminescence devices using the low work function cathode.
 [DOI: 10.1063/1.1925311]

Since the observation of intensive visible light emission from porous silicon at room temperature,[1] silicon nanostructures have received enormous interest and have been studied intensively for their potential applications in optoelectronics devices.[2,3] The origin of visible light emission in porous Si remains under debate. Silicon nanostructure was originally believed to be responsible for the radiative recombination. Nevertheless, theoretical investigations further showed that the rupture of the translational symmetry in silicon nanostructure could cause the transition from indirect to direct band gaps, with a large increase in the probability of radiative recombination.[4] Many problems remain to be solved in using porous Si for practical applications, such as the low efficiency in light emission under a bias, the instability of light emission due to spontaneous oxidation at ambient conditions, the sensitivity of luminescence to the preparation conditions, and the fragility in mechanical properties, etc.[5]

As an indirect band gap material, bulk Si is known to be inefficient in light emission. Besides, the low band gap of bulk Si at about 1.1 eV allows only for infrared emission, instead of visible light. Therefore, optoelectronic devices are currently built on compound semiconductors due to their high efficiency in light emission. Compound semiconductors, however, are hard to integrate into cheap and versatile silicon circuits due to lattice mismatch problems. Once Si devices can be made exhibiting high electroluminescence (EL) efficiency, the low cost and powerful optoelectronic integrated circuit Si devices will become feasible. Besides, due to mature processing technologies, the Si-based light-emitting diode (LED) may become a candidate for the next generation flat-panel display. Since the Si nanostructure has been believed to be responsible for the visible light emission in porous Si, various techniques have been attempted to improve the fabrication of Si nanostructures, including chemical vapor deposition,[6] sputtering,[7] Si ion implantation into SiO_2 films,[8] cluster ion-beam deposition,[9] laser ablation,[10] etc.

Recently, silicon nanocrystals (Si-NCs) embedded in a silica (SiO_x) matrix have been demonstrated to emit visible light by photoluminescence (PL) measurements. Sufficiently high efficiency of visible light emission with various colors could be observed from the Si-NCs/a-SiO_x composites, and the PL intensity was high enough for LED applications.[6,8,11] However, only a few papers have reported on the electroluminescence characteristics of Si-NCs/a-SiO_x,[12–14] mainly due to the difficulty of the tunneling of electrons and holes through the wide band gap oxide and their efficient optical recombination within the nanocrystals. Thus, silicon nitride, rather than oxide, is attempted as the matrix material due to its lower band gap for tunneling.

In this study, the optoelectronic nanocomposite films were deposited on Si (100) and indium tin oxide (ITO) glass substrates at room temperature by e-beam evaporation of Si into the inductively coupled plasma (ICP) in N_2/H_2 gases. The deposited Si-NCs/a-SiN_x films were employed as the active layer. Figure 1 shows the PL spectra of the films deposited at various gaseous N_2/H_2 ratios. A Xe lamp operated at 150 W was employed as the excitation source for the PL spectra. The wavelength of excitation is 325 nm. The PL spectra show that the positions of emission peaks are insensitive to the N_2/H_2 ratios. However, the intensity reaches the maximum when the nitrogen is at 50% in the N_2/H_2 mixture. When starting to increase N_2 in H_2, the interface between silicon nitride and silicon starts to appear with the interface passivated by hydrogen, so that the PL intensity is enhanced. However, when increasing nitrogen above 50%, the ionization of nitrogen becomes low and the hydrogen passivation is also reduced, so that the PL intensity is decreased. In addition, the emission peak can be deconvoluted into two broad peaks at 2.7 and 3.0 eV.

[a]Electronic mail: sampras@mail.ncku.edu.tw
[b]Electronic mail: hong@mail.ncku.edu.tw

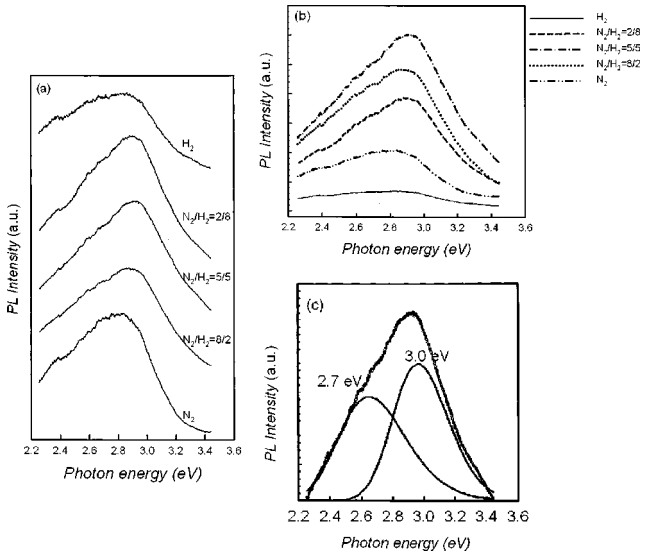

FIG. 1. (a) PL spectra of the films deposited at various N_2/H_2 ratios, (b) the intensity of photoluminescence as a function of nitrogen composition in the gas, and (c) the deconvolution of PL spectra at $N_2/H_2=5/5$ into two peaks: 2.7 and 3.0 eV.

Since the band gap of bulk silicon is only 1.1 eV, the observed high-energy values of emission peaks at 2.7 and 3.0 eV are likely due to the quantum confinement effect (QCE) from ultrafine nanoparticles. Figure 2 shows the image from high-resolution analytical electron microscopy (HRAEM). Si-NCs were clearly observed to be embedded in amorphous silicon nitride matrix. The sizes of Si-NCs were in the range of 1–5 nm, and the density of Si-NCs was about 5×10^{12} cm^{-2}. The selective area diffraction ring confirmed the formation of Si crystallites. The nitrogen element mapping of the film was further obtained using electron energy loss spectroscopy (EELS) by measuring the N *K* edge at 400 eV. By comparing the EELS energy filter image with the corresponding transmission electron microscope (TEM) image, Si-NCs were clearly observed to be embedded in the silicon nitride matrix. Assuming spherical Si nanocrystals with finite barrier height and effective electron mass $m_e^*=0.15m_0$, the band gap energy can be shifted to 2.7 or 3.0 eV when the Si crystal size reduces to 1–2 nm due to the QCE.

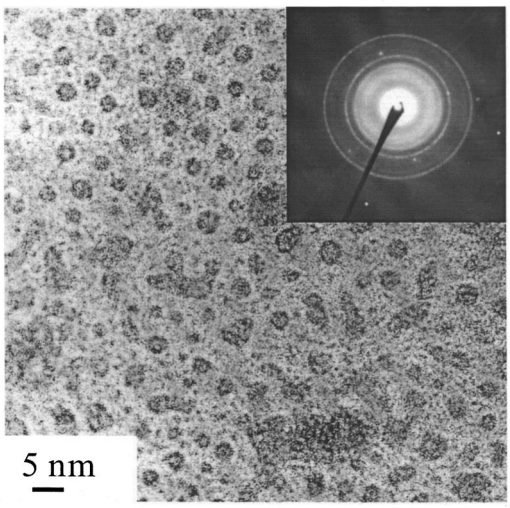

FIG. 2. HRAEM image of the Si-NCs/*a*-SiN_x nanocomposite. The inset shows a selective area diffraction pattern of Si nanocrystals.

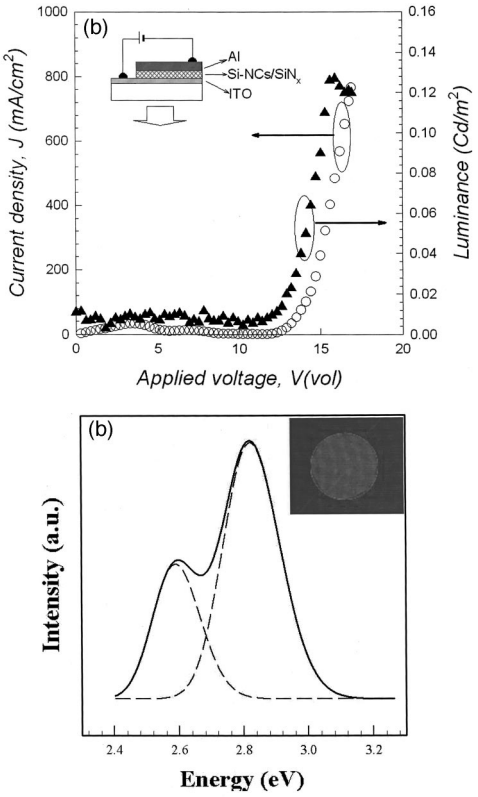

FIG. 3. (a) The characteristics of the current density (J) and the luminance (L) versus the forward bias voltage (V) for the Si-NCs/*a*-SiN_x film with the Al cathode measured at room temperature, and (b) the corresponding EL spectrum. The inset in (b) is the photograph of EL device emission. The diameter of the pattern is about 2 mm.

On the other hand, the emission peaks at 2.7 and 3.0 eV might also be ascribed to the electronic transitions of the interface states, $\equiv Si\rightarrow =N^-$ and $Si^\circ\rightarrow E_v$, as calculated by Robertson *et al.*[15] and experimentally verified by Mo *et al.*[16] The active centers for light emission at 2.7 and 3.0 eV were not clear, either in the ultrafine nanoparticles around 1–2 nm or at the interface between Si nanocrystal and silicon nitride matrix.

The structure of the EL device was glass/ITO/Si-NCs/Al. The thickness of the active layer measured by cross-sectional TEM was about 20 nm. In this study, we employed the ITO substrate as the anode and used a metal electrode as the cathode. The current density-voltage (J-V) characteristics of the EL device under the forward bias are shown in Fig. 3(a). The ITO anode was positively biased and the metal cathode was negatively biased. The Si-NCs/*a*-SiN_x device exhibited significantly higher current densities (800 mA/cm^2) and electroluminescence intensities (0.12 Cd/m^2) than did the Si-NCs/*a*-SiO_x devices. The EL spectra were measured using a double-grating monochromator with a charge-coupled diode detector. The EL spectrum, shown in Fig. 3(b), was deconvoluted into two broad peaks centered around 2.5 and 2.8 eV. The positions of two peaks are very close to those of the PL peaks.

The effects of the cathode material, Al or Ca/Ag, on the current density and luminescence of the EL devices are also shown in Fig. 4. For the device with Al cathode, the turn-on voltage was around 14 V, above which the current density and luminance began to rise sharply. The maximal luminance was 0.12 Cd/m^2, and the maximal EL efficiency achieved

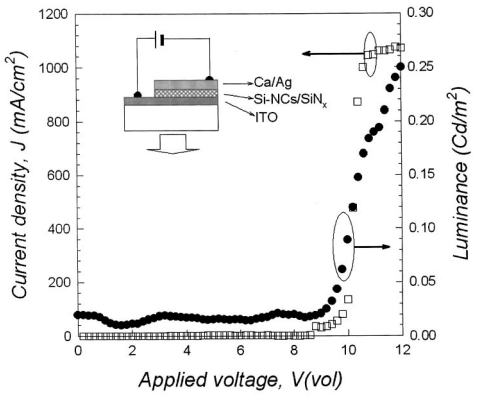

FIG. 4. The characteristics of the current density (J) and the luminance (L) versus the forward bias voltage (V) for the Si-NCs/a-SiN_x film with the Ca/Ag cathode measured at room temperature.

was about 6×10^{-4} Cd/A. By replacing Al with a Ca/Ag cathode, the turn-on voltage could be reduced to 10 V, and the maximal luminance was increased to 0.25 Cd/m^2. The maximal EL efficiency achieved was 1.6×10^{-1} Cd/A, much higher than that for the Al cathode. Even at the maximal luminance, the Ca/Ag cathode still outperformed the Al cathode (e.g., luminance: 0.25 versus 0.12 Cd/m^2, current density: 10.5 versus 7.8×10^3 A/m^2, voltage: 10 versus 14 V). Evidently, the Ca/Ag cathode improved the device performance by simultaneously increasing the current density, the maximal luminance, and the EL efficiency.

Here, we deduced that the device performance should be dependent on the work function of the cathode material. The work functions of Ca/Ag and Al are 2.8 and 4.3 eV, respectively. The electrons' injection from the Ca/Ag cathode to the lowest unoccupied molecular orbital states at nanocrystals is easier than that from the Al cathode due the lower energy barrier. Therefore, the current density and EL efficiency of the device with Ca/Ag cathode are higher than those with the Al cathode. As suggested from the results just presented, the light emission mechanism in our devices is dominated by the injection of electrons and holes from the cathode and anode, respectively, and relies much less on the excitation of hot electron carriers by a high electric field. This conclusion is further supported by our observation that no light was emitted from the device under a reverse bias. In our devices, ITO also played an important role in injecting the holes into the highest occupied molecular orbital states at nanocrystals owing to its high work function of 4.7 eV. Our results suggest that the EL efficiency of the Si-NCs can be further improved by choosing appropriate cathode and anode materials.

In summary, Si-NCs were deposited by electron-gun evaporation of Si into the ICP of N_2/H_2 in order to control the sizes of nanocrystals. In the PL spectra, the main emission is a blue band (3.0 eV) for the Si-NCs/a-SiN_x nanocomposite film. The emission wavelength is much shorter than those (1.5–1.8 eV, red band) reported in the literature.[17] For the EL devices containing Si-NCs/a-SiN_x, the J-V curves exhibit diode characteristics. The EL efficiency of the Si-NCs/a-SiN_x device was also dependent on the cathode and anode materials used. The Ca/Ag cathode outperformed the Al cathode by simultaneously increasing the current density, the maximal luminance, and the EL efficiency of the device. The ITO anode was essential for the hole injection owing to its high work function. For the EL device using ITO, Si-NCs/a-SiN_x and Ca/Ag as the anode, active layer, and cathode, respectively, the emission was observable with the naked eye through the ITO glass in the dark.

The authors are grateful for assistance from L. C. Wang for HRAEM analysis and Professor W. Chen for photoluminescence measurement. The support for this work from National Science Council, under contract no. NSC-93-2811-E-006-018, contract, and Center for Micro-Nano Technology, National Cheng Kung University is gratefully acknowledged.

[1] L. T. Canham, Appl. Phys. Lett. **57**, 1046 (1990).
[2] L. T. Canham, Nature (London) **408**, 411 (2000).
[3] L. Pavesi, L. D. Negro, C. Mazzoleni, G. Franzo, and F. Priolo, Nature (London) **408**, 440 (2000).
[4] L. Brus, J. Phys. Chem. **98**, 3575 (1994); S. S. Iyer and Y. H. Xie, Science **260**, 40 (1993); T. Takagahara and K. Takeda, Phys. Rev. B **46**, 15578 (1992).
[5] M. A. Tischler, R. T. Collins, J. H. Stathis, and J. C. Tsang, Appl. Phys. Lett. **60**, 639 (1992).
[6] N.-M. Park, T.-S. Kim, and S.-J. Park, Appl. Phys. Lett. **78**, 2575 (2001); B. H. Augustine, E. A. Irene, Y. J. He, K. J. Price, L. E. McNeil, K. N. Christensen, and D. M. Maher, J. Appl. Phys. **76**, 4020 (1995); D. J. Dimaria, J. R. Kertley, E. J. Pakulis, D. W. Dong, T. S. Kuan, F. L. Pesavento, T. N. Theis, J. A. Cutro, and S. D. Brorson, *ibid.* **56**, 401 (1984); J. F. Tong, H. L. Hsiao, and H. L. Hwang, Appl. Phys. Lett. **74**, 2316 (1999).
[7] S. Furukawa and T. Miyasato, Jpn. J. Appl. Phys. **27**, L2207 (1988).
[8] T. S. Iwayama, S. Nakao, and K. Saitoh, Appl. Phys. Lett. **65**, 1814 (1994); L.-S. Liao, X.-M. Bao, X.-Q. Zhang, N.-S. Li, and N.-B. Min, *ibid.* **68**, 850 (1996); K. Lutervá, T. Pelant, I. Mikulskas, R. Tomasiuas, D. Muller, J.-J. Grob, J.-L. Rehspringer, and B. J. Hönerlage, J. Appl. Phys. **91**, 2896 (2002).
[9] M. Ehbrecht, B. Kohn, F. Huisken, M. A. Laguna, and V. Paillard, Phys. Rev. B **56**, 6958 (1997); G. Ledoux, J. Gong, and F. Huisken, Appl. Phys. Lett. **79**, 4028 (2001).
[10] L. Patrone, D. Nelson, V. I. Safaov, M. Sentis, W. Marine, and S. Giorgio, J. Appl. Phys. **87**, 3829 (2000).
[11] Y. Kanemitsu, T. Ogawa, K. Shiraishi, and K. Takeda, Phys. Rev. B **48**, 4883 (1993); L. Meda, E. Grilli, and M. Guzzi, Appl. Phys. Lett. **66**, 851 (1995); J.-J. Wu, T.-C. Wong, and C.-C. Yu, Adv. Mater. (Weinheim, Ger.) **12**, 1643 (2002).
[12] G. Franzò, A. Irrera, E. C. Moreira, M. Miritello, F. Iacona, D. Sanfilippo, G. Di Stefano, P. G. Fallica, and F. Priolo, Appl. Phys. A: Mater. Sci. Process. **74**, 1 (2002).
[13] P. Photopoulos and A. G. Nassiopoulou, Appl. Phys. Lett. **77**, 1816 (2000).
[14] K. Luterová, I. Pelant, J. Valenta, J.-L. Rehspringe, D. Muller, J. J. Grob, J. Dian, and B. Hönerlage, Appl. Phys. Lett. **77**, 2952 (2000).
[15] J. Robertson and M. J. Powell, Appl. Phys. Lett. **44**, 415 (1984).
[16] C. M. Mo, L. Zhang, C. Xie, and T. Wang, J. Appl. Phys. **73**, 5185 (1993).
[17] A. P. Li, I. Zhang, Y. X. Zhang, G. G. Qin, X. Wang, and X. W. Hu, Appl. Phys. Lett. **69**, 4 (1996); K. Chen, M. Wang, W. Shi, L. Jiang, W. Li, J. Xu, and X. Huang, J. Non-Cryst. Solids **198**, 833 (1996); G. F. Bai, Y. P. Qiao, Z. C. Ma, W. H. Zong, and G. G. Qin, Appl. Phys. Lett. **72**, 3408 (1998).